

OPEN ACCESS

Passivation of Zinc Oxide Nanowires for Improved Piezoelectric Energy Harvesting Devices

To cite this article: Nimra Jalali *et al* 2013 *J. Phys.: Conf. Ser.* **476** 012131

View the [article online](#) for updates and enhancements.

You may also like

- [Highly efficient bifacial semitransparent perovskite solar cells based on molecular doping of CuSCN hole transport layer](#)
Shixin Hou, , Biao Shi et al.
- [Characterization of Fe doped n-CuSCN/p-Cu₂S solid-state photovoltaic cell](#)
S P A U K Samarakoon, P G D C K Karunaratna and C A N Fernando
- [Microstructures, optical and photovoltaic properties of CH₃NH₃PbI_{3-x}Cl_x perovskite films with CuSCN additive](#)
Yasuhiro Shirahata and Takeo Oku



UNITED THROUGH SCIENCE & TECHNOLOGY

 **The Electrochemical Society**
Advancing solid state & electrochemical science & technology

**248th
ECS Meeting**
Chicago, IL
October 12-16, 2025
Hilton Chicago

**Science +
Technology +
YOU!**

**SUBMIT
ABSTRACTS by
March 28, 2025**

SUBMIT NOW

Passivation of Zinc Oxide Nanowires for Improved Piezoelectric Energy Harvesting Devices

Nimra Jalali¹, Joe Briscoe¹, Peter Woolliams², Mark Stewart², Paul M. Weaver², Markys Cain² and Steve Dunn¹

¹Queen Mary University of London, ²National Physical Laboratory

Email: s.c.dunn@qmul.ac.uk

Abstract. This paper evaluates the improvement in performance of ZnO nanowires energy harvesters using p-type copper thiocyanate (CuSCN) passivation. Two types of p-n junction based devices: ZnO/PEDOT:PSS (poly(3,4-ethylene-dioxythiophene) poly(styrenesulfonate)) and ZnO/CuSCN/PEDOT:PSS were fabricated. It was observed that, the passivation of nanowires using CuSCN improved the performance four times, yielding a peak power density of $303 \mu\text{Wcm}^{-2}$ for a load of 3.54 k Ω . The results were supported by impedance analysis of each device and it was observed that the piezoelectric voltage output of the device depends on its RC time constant.

1. Introduction

Energy harvesting from ambient sources is a potential substitute to conventional power generation methods. In order to deal with energy supply and storage issues, research work has developed promising macro-power and micro-power energy harvesting systems. In case of micro-power energy harvesters, piezoelectric devices combine the ability of being self-powered with size compactness[1]. MEMS (Micro-Electro-Mechanical Systems) piezoelectric systems are commercially applied as sensors and detectors for navigation, automotive and smartphones[2][3]. They have gained wide attention in wireless sensing and monitoring for remote operations of systems on which wired connections are impractical[4][5]. The most commonly used piezoelectric material is lead zirconate (PZT). PZT has k_{33} electromechanical coupling coefficient of ≈ 0.67 [6] but, being brittle in nature, it has limitations in applications[7].

The piezoelectric voltage measurement of ZnO nanowires was demonstrated in 2006[8]. Since then, it became an attractive material for nanostructure-based piezoelectric energy harvesters. The Young's Modulus of ZnO nanowires, has been reported to be up to 100 GPa[9], which can make it withstand loadings higher than PZT. ZnO nanogenerator energy harvesters have been fabricated with Schottky contacts[10], insulator contacts[11] and p-n junctions[12]. ZnO is an n-type semiconductor and allows mobile charges to flow under piezoelectric voltage. These charges internally screen the polarization field[12]. In addition, external screening of the field occurs through contact of ZnO with metals and metal oxides[12]. ZnO has intrinsic surface donor defects such as oxygen vacancies and zinc interstitials[13][11]. The interaction of the material surface with moisture creates hydroxyl OH⁻ ions which were also identified as donor species[14]. These defect states reduce the piezoelectric voltage by screening the polarization charges[11][15]. Therefore, surface modification techniques have been applied previously[11][15] to suppress their effect. In this paper, passivation technique using p-type CuSCN is reported. The observations are supported by impedance analysis results. Two



devices comprising of ZnO/PEDOT:PSS and ZnO/CuSCN/PEDOT:PSS were fabricated. The effect of screening rate on the voltage output was studied using the RC time constant of the devices.

2. Method

ZnO nanowires were grown on flexible indium-tin oxide (ITO)-coated polyethylene terephthalate (PET) substrates ($2 \times 1 \text{ cm}^2$) using aqueous solutions of $0.025 \text{ M Zn(NO}_3)_2 \cdot 6\text{H}_2\text{O}$ and 0.025 M hexamethylenetetramine at 90°C [12]. For the ZnO/CuSCN/PEDOT:PSS device, the nanowires were spray-deposited with 5 ml of 0.15 M CuSCN solution in dipropyl sulphide using a method described elsewhere [16]. Both the CuSCN-passivated and non-CuSCN-passivated nanorods were thermally treated at 50°C for 44 hours. For passivated nanowire, thermal treatment evaporated dipropyl sulphide. Whereas, for the non-CuSCN passivated nanowires, it was performed to analyze the output difference from our previously reported PEDOT:PSS device[17]. Two layers of PEDOT:PSS were spin-coated at 2000 RPM for 30 seconds onto the nanowires (Figure 1(d)). After deposition, each layer was dried at 100°C . A gold electrode was sputtered on top of PEDOT:PSS. Copper wires were connected as extensions to ITO and gold electrodes. The $2 \times 1 \text{ cm}^2$ device was mounted on a $500 \mu\text{m}$ thick plastic substrate. One end of the substrate was displaced to $\approx 6 \text{ mm}$ using a cam connected to rotating motor shaft. The other end was fixed to a sample holder[17]. The generated voltage was measured under open-circuited conditions and across load resistances using NI-PXIe 1062Q and Meatest M602 programmable decade box. Short-circuit current was measured using Low-Noise Current Preamplifier SR570. Impedance analysis was carried out using 4294a Agilent Impedance Analyzer.

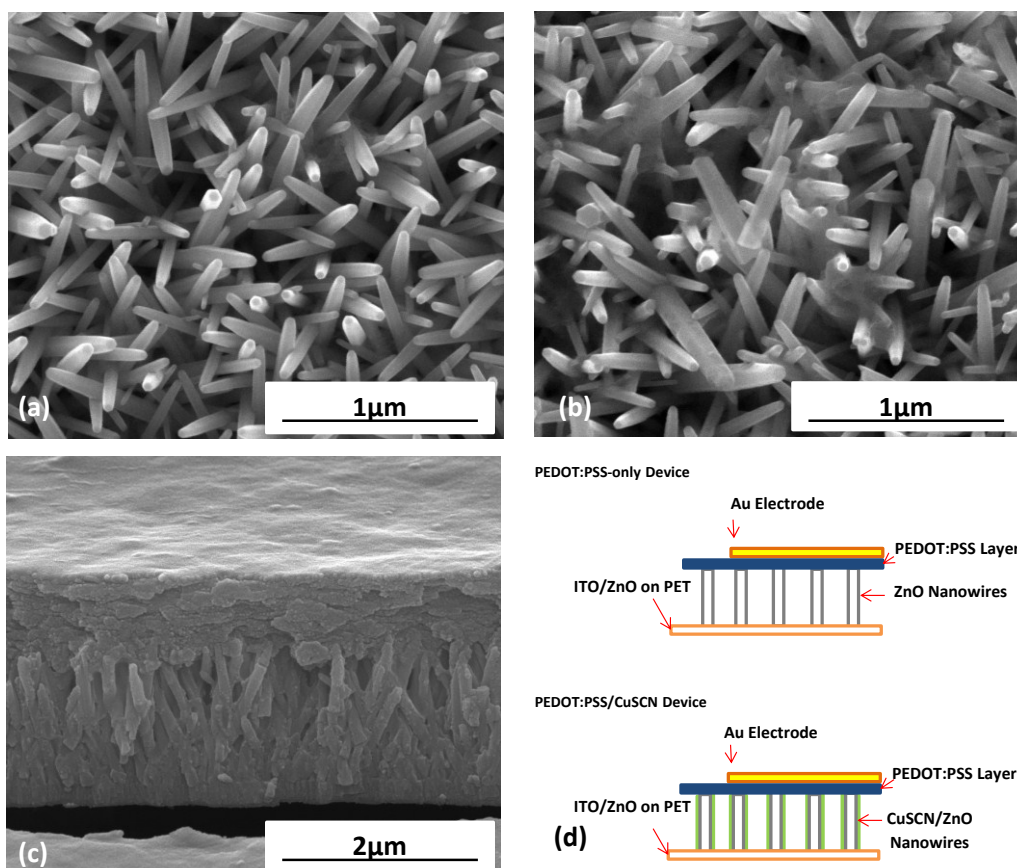


Figure 1. SEM Images: ZnO nanowires (a) ZnO nanowires with CuSCN deposition (b) PEDOT:PSS layer on top of ZnO nanowires (c). Schematic of ZnO/PEDOT:PSS and ZnO/CuSCN/PEDOT:PSS devices (d).

3. Results and Discussion

Vertical c-axis oriented ZnO nanorods having ≈ 70 nm thickness and ≈ 2 μm length are shown in Figure 1(a). The nanowires were not grown in closely packed fashion and were tilted due to seed layer texturing. As shown in Figure 1(b), the nanowire arrays were coated with CuSCN along the length. The spray coating technique was used to control the amount of deposition. Figure 1(c) shows, ZnO/PEDOT:PSS junction with PEDOT:PSS layer settled on top of the nanowires.

A ZnO/PEDOT:PSS device with thermal treatment generated an open-circuit voltage of ≈ 225 mV (Figure 1(a)) which was twice the voltage of our previously reported unannealed ZnO based PEDOT:PSS device[17]. This performance improvement could be related to the removal of surface adsorbed OH⁻ ions and chemical precursor material. ZnO has six times improved voltage output when annealed at 350°C[15], which may also be due to an annealing-induced reduction in oxygen vacancies[18]. The peak voltage output of the ZnO/CuSCN/PEDOT:PSS device was ≈ 673 mV (Figure 1(c)). This is a combined effect of thermal and CuSCN passivation of the device defect states on nanowire surface. ZnO has a number of surface defects. They include oxygen defects, which have been identified as the cause of the green emissions in the nanorods[13], and the moisture-generated OH⁻ ions[14]. They are the main donor species found on ZnO surface[14] and therefore they tend to increase the conductivity of ZnO[15]. This leads to increase in internal screening of polarization charges. Surface passivation reduces the parasitic activity of surface defects which causes a decrease in defect-induced carrier density in ZnO[11]. Therefore, the rate of internal screening reduces and voltage across piezoelectric ZnO improves.

The power density of ZnO/CuSCN/PEDOT:PSS was obtained as 303 μWcm^{-2} across an optimal load resistor of 3.54 k Ω (Figure 2(e)) which was approximately four times higher than the ZnO/PEDOT:PSS device. The Nyquist impedance representation is indicative that, CuSCN passivation improved the internal resistance. The real axis semi-circle diameter of the Nyquist plot for ZnO/CuSCN/PEDOT:PSS was ≈ 10 k Ω as compared to ≈ 2.5 k Ω for ZnO/PEDOT:PSS (Figure 3). This correlates with a higher optimum load point for the ZnO/CuSCN/PEDOT:PSS device (Figure 2(e)). As observed from the impedance response, the devices can be modeled as RC circuits with their charge and discharge time constants determined by $\tau = RC$ ($\tau = f_c^{-1}$)[19] (Figure 3). Evidently, for the ZnO/PEDOT:PSS device the time constant was 0.55 ms which increased to 2.28 ms with the deposition of CuSCN. This indicated the increase in charge storage in the piezoelectric device and decrease in screening rate. This agrees with the proposed reduction in screening rate achieved by CuSCN passivation of the ZnO surface, which could account for the higher peak voltage and power output.

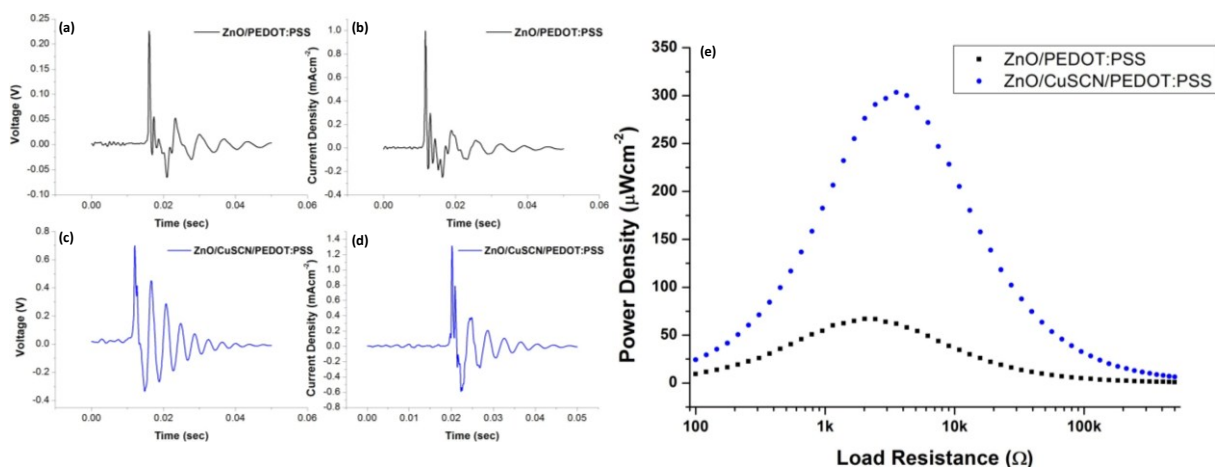
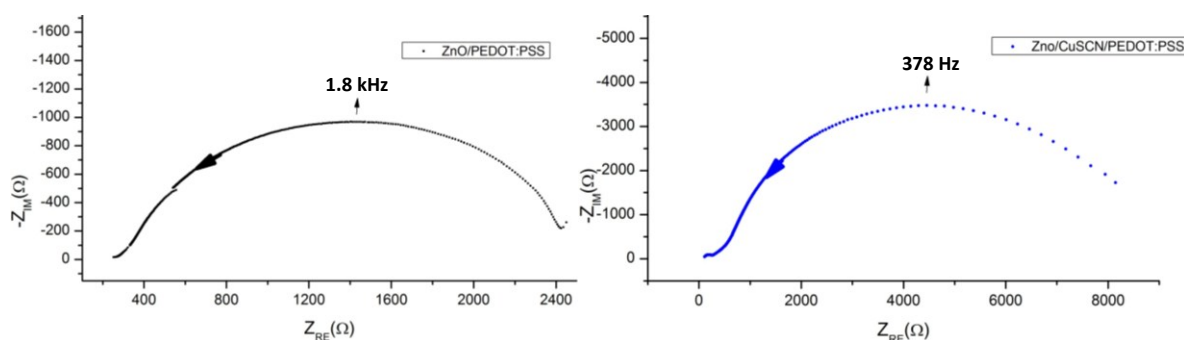


Figure 2. Performance measurement: open-circuit voltage (a) and short circuit current density (b) of ZnO/PEDOT:PSS device, open-circuit voltage (c) and short-circuit current density (d) of ZnO/CuSCN/PEDOT:PSS device, (e) load curves of ZnO/PEDOT:PSS and ZnO/CuSCN/PEDOT:PSS device showing power density at optimum load resistance.

Table 1. Performance parameters of ZnO/PEDOT:PSS and ZnO/CuSCN/PEDOT:PSS devices.

Device	Open Circuit Voltage	Short Circuit Current	Load Resistance	Voltage On Load Resistance	Current Density On Load Resistance	Power Density
	mV	mAc ^m - ²	k Ω	mV	mAc ^m - ²	μ Wcm ⁻²
ZnO/PEDOT:PSS	225	1.00	2.00	114	0.58	66.80
ZnO/CuSCN/PEDOT:PSS	673	1.30	3.54	389	0.78	303.39

**Figure 3.** Nyquist plot obtained from impedance analysis (40 Hz-110 MHz) of ZnO/PEDOT:PSS (a) and ZnO/CuSCN/PEDOT:PSS (b) devices.

4. Conclusion

A suitable passivation technique was adopted which improved the energy harvester's power density from ≈ 66 to $\approx 303 \mu\text{Wcm}^{-2}$ across an optimum load resistor.

This work demonstrates the importance of impedance analysis for energy harvester optimization. It unfolded important relation between circuit behaviour and rate of screening. The voltage build-up across ZnO nanowires was found to be related to the RC time constant of the devices. This supports the explanation that surface defects and impurities increase the screening effect in piezoelectric ZnO. Passivation reduced the parasitic effects and improved circuit time constant from ≈ 0.55 to ≈ 2.28 ms.

References

- [1] Uchino K 2008 Piezoelectric Motors and Transformers *Piezoelectricity SE - 11* vol 114 (Springer Berlin Heidelberg) pp 257–77
- [2] Marek J 2011 Automotive MEMS sensors — Trends and applications *Proceedings of 2011 International Symposium on VLSI Technology, Systems and Applications* (IEEE) pp 1–2
- [3] Lim H J, Singh R P, Chuan K C T, Nuttman D and Je M 2011 Double regulated voltage supply for high precision MEMS accelerometers *2011 International Symposium on Integrated Circuits* (IEEE) pp 571–4
- [4] James E P, Tudor M J, Beeby S P, Harris N R, Glynne-Jones P, Ross J N and White N M 2004 An investigation of self-powered systems for condition monitoring applications *Sensors Actuators A Phys.* **110** 171–6
- [5] Lallart M, Guyomar D, Jayet Y, Petit L, Lefeuvre E, Monnier T, Guy P and Richard C 2008 Synchronized switch harvesting applied to self-powered smart systems: Piezoactive microgenerators for autonomous wireless receivers *Sensors Actuators A Phys.* **147** 263–72
- [6] Priya S and Nahm S 2012 *Lead-Free Piezoelectrics* (New York, NY: Springer New York)
- [7] Anton S R and Sodano H A 2007 A review of power harvesting using piezoelectric materials (2003–2006) *Smart Mater. Struct.* **16** R1–R21

- [8] Wang Z L and Song J 2006 Piezoelectric nanogenerators based on zinc oxide nanowire arrays. *Science* **312** 242–6
- [9] Hoffmann S, Östlund F, Michler J, Fan H J, Zacharias M, Christiansen S H and Ballif C 2007 Fracture strength and Young's modulus of ZnO nanowires *Nanotechnology* **18** 205503
- [10] Xu S, Qin Y, Xu C, Wei Y, Yang R and Wang Z L 2010 Self-powered nanowire devices. *Nat. Nanotechnol.* **5** 366–73
- [11] Hu Y, Lin L, Zhang Y and Wang Z L 2012 Replacing a battery by a nanogenerator with 20 V output. *Adv. Mater.* **24** 110–4
- [12] Briscoe J, Stewart M, Vopson M, Cain M, Weaver P M and Dunn S 2012 Nanostructured p-n Junctions for Kinetic-to-Electrical Energy Conversion *Adv. Energy Mater.* **2** 1261–8
- [13] Lv Y, Yao W, Ma X, Pan C, Zong R and Zhu Y 2013 The surface oxygen vacancy induced visible activity and enhanced UV activity of a ZnO_{1-x} photocatalyst *Catal. Sci. Technol.*
- [14] Liu W Z, Xu H Y, Ma J G, Liu C Y, Liu Y X and Liu Y C 2012 Effect of oxygen-related surface adsorption on the efficiency and stability of ZnO nanorod array ultraviolet light-emitting diodes *Appl. Phys. Lett.* **100** 203101
- [15] Pham T T, Lee K Y, Lee J-H, Kim K-H, Shin K-S, Gupta M K, Kumar B and Kim S-W 2013 Reliable operation of a nanogenerator under ultraviolet light via engineering piezoelectric potential *Energy Environ. Sci.* **6** 841
- [16] Hatch S M, Briscoe J, Sapelkin A, Gillin W P, Gilchrist J B, Ryan M P, Heutz S and Dunn S 2013 Influence of anneal atmosphere on ZnO-nanorod photoluminescent and morphological properties with self-powered photodetector performance *J. Appl. Phys.* **113** 204501
- [17] Briscoe J, Jalali N, Woolliams P, Stewart M, Weaver P M, Cain M and Dunn S 2013 Measurement techniques for piezoelectric nanogenerators *Energy Environ. Sci.* **6** 3035
- [18] Kushwaha A, Tyagi H and Aslam M 2013 Role of defect states in magnetic and electrical properties of ZnO nanowires *AIP Adv.* **3** 042110
- [19] Keawboonchuay C and Engel T G 2003 Electrical power generation characteristics of piezoelectric generator under quasi-static and dynamic stress conditions *IEEE Trans. Ultrason. Ferroelectr. Freq. Control* **50** 1377–82